A Multifrequency Multistage Fingerprinting-based Radiolocation System

Murat Ambarkutuk
Mechanical Engineering Department,
Virginia Polytechnic Institute and State University,
Blacksburg, Virginia, USA Email:murata@vt.edu

Tomonari Furukawa
Mechanical Engineering Department,
Virginia Polytechnic Institute and State University,
Blacksburg, Virginia, USA Email: tomonari@vt.edu

Abstract*—This paper presents a multifrequency and multistage indoor fingerprinting-based radiolocation system. The proposed system relies on a 900 MHz and with 2.4 GHz radios based on 802.15.4 protocol. By exploiting different propagation characteristics of different Radio Frequency (RF) signal wave within a Gated Recurrent Unit (GRU) framework, Received Signal Strength (RSS) and Round Trip Time (RTT) measurements are used for indoor localization purposes. Similar to conventional fingerprinting systems, the system is consisted of two phases: data acquisition and learning (offline), and localization (online). In offline phase, the propagation function for each Anchor Node (AN) and path loss exponent is learned by a recurrent network consisted of GRU from RSS and RTT measurements, whereas the online phase contains different stages of localization and an information fusion stage. *Add some result once get it

I. Introduction

Inverse pyramid:

- P1: Background
  1) Inverse pyramid
  2) Last sentence: introduce the area of the title of your paper as a significant topic
  3) 5 refs (books, review papers, journals, no conf)
- P2-3: Background
  1) Original classification: Support the objectives with each sentence
  2) Appreciate their work, their focus however different
  3) no technical words
  4) 10 refs (journal, conference papers)
- P4: Objectives
  1) 1-3 objectives
  2) the first sentence: this paper presents

The organization of the paper as follows. Section II lays out the fundamentals of the radio wave propagation, while Section III covers the details of the proposed system. Section IV demonstrates the validity of the proposed system in different environments. In Section V, the experimentation results will be concluded and future work will be addressed.

II. Radio Wave Propagation in Radiolocation and Function Approximation

This section will cover the fundamentals of radio wave propagation in the context of Fingerprinting-based Indoor Radiolocation Systems (FIRL). FIRLs consist of two main phases. The first phase, i.e. offline phase, involves the collection of some types measurements from n_{an} number Anchor Node (AN) placed in the environment. The measurements and the corresponding positions where the measurements are taken form measurement space $\boldsymbol{M} \in \mathbb{R}^{n_s \text{ x } n_a}$ and localization space $\boldsymbol{X} \in \mathbb{R}^{n_s \text{ x } 3}$ Let $m_j^i \in \mathbb{Z}^1$ and $d_j^i \in \mathbb{R}^1$ be the measurement obtained from anchor node i at location j, and the radial distance between location j and anchor node i, respectively. The measurement space $\boldsymbol{m}^i = \{m_j^i | j = 1 \dots n_{loc}\} \in \mathbb{R}^{n_{loc}}$ is often constructed in either frequency domain [refer CSI], or time domain. The measurements are then used to approximate the propagation function $f_d^i : \mathbb{Z}^1 \mapsto \mathbb{R}^1$ of anchor node i. Figure 1 illustrates the localization environment and the robot pose etc.

The fundamental problem of radiolocation systems can be seen as an function approximation problem where $\hat{f} : \boldsymbol{M} \mapsto \boldsymbol{X}$ the approximated propagation function is used to project fingerprints to estimated positions, or even pose.

$$f_d^i(m_j^i) = d_j^i \tag{1}$$

One of the most popular fingerprints is Received Signal Strength (RSS) in FIRLs due to its simplicity in fingerprint acquisition during the surveying. The fundamental relationship between transmitted and received signal strengths P_t and $P_r(d)$ between ideal antennas in an empty space with a separation distance d is characterized by Friis' Free Space Equation (FFSE), given below [1].

$$P_r(d) = \frac{P_t G_t G_r \lambda^2}{(4\pi d)^2 L} \tag{2}$$

In Equation (2), G_t and G_r denote the unitless gains of transmitter and receiver antennas, respectively, whereas λ is the wavelength of the radio wave. Moreover, since the received signal strength is often at a minuscule level, the FFSE is denoted in the decibel scale relative to a milliwatt.

$$\begin{aligned}\widetilde{P}_r(d) = \widetilde{P}_t + 10\log G_t + 10\log G_r + \\ 20\log\lambda - 20\log d - 20\log 4\pi\end{aligned} \tag{3}$$

$\widetilde{P}_r(d)$ and $\widetilde{P}_t$ represent received and transmitted signal strengths in the decibel scale. Although, neither Equation (2) nor Equation (3) holds true for the distance $0 < d < \lambda$.

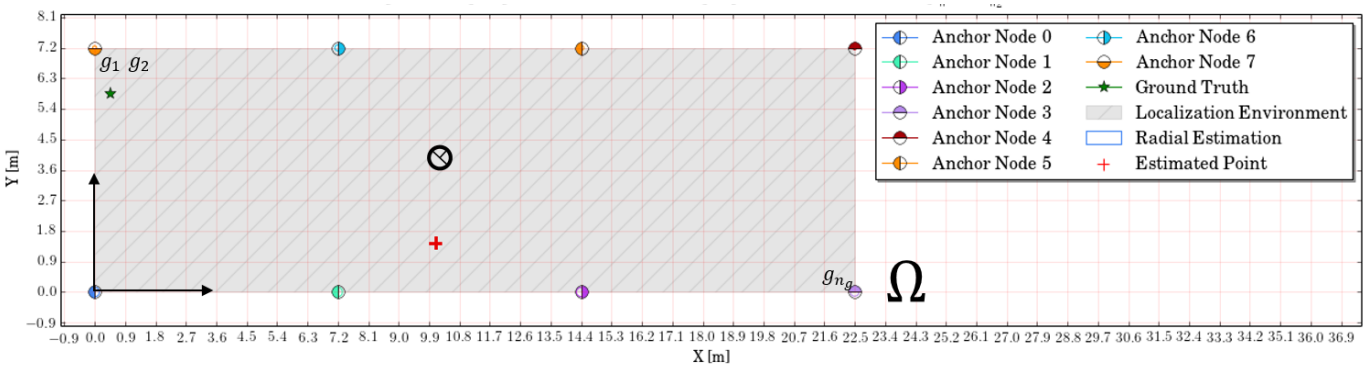

Fig. 1: Localization Environment

Thus, received signal strength is generally denoted relative to a reference point d_0 with a prior corresponding received signal strength.

$$\widetilde{P}_r(d) = \widetilde{P}_r(d_0) + 20 \log \frac{d_0}{d} \tag{4}$$

However well-known, neither the FFSE nor its variants are able to model major propagation mechanisms, i.e. reflection, diffraction or scattering occurring along the the propagation path, due to the fact that it can only model Line-of-sight (LOS) propagation. Thus, it is often impractical to utilize the FFSE in indoor localization problems where reflection and diffraction occurs along the propagation path. The energy loss occurring along the propagation path which can be derived as the difference between transmitted and received signal strength should incorporate the loss occurring LOS propagation with other losses due to the structure of the environment. Equation (5) represents a special Path Loss (PL) model, i.e. Log-distance Path Loss (LDPL) which describes the attenuation relative to a reference point as the sum of the LOS propagation losses and the losses resulted by the structure of the environment. One of the major advantages of the LDPL model over the the FFSE is that the LDPL model can account for obstructions and corresponding wave propagation in the space with varying values of PL exponent n.

$$\overline{PL}(d) = \overline{PL}(d_0) + 10n \log \frac{d}{d_0} \tag{5}$$

$$n = \begin{cases} < 2, & \text{if the space structure guides the radio waves along the propagation path,} \\ = 2, & \text{if the space is empty,} \\ > 2, & \text{if there are obstructions along the propagation path.} \end{cases} \tag{6}$$

One of the most common solution in FIRLs is to estimate n by fitting a curve to collected fingerprints. Given a mean PL at an unknown location $\overline{PL}(d)$, PL exponent n and a mean PL at the reference point d_0 $\overline{PL}(d_0)$, the propagation function of anchor node i f_d^i can be obtained by solving the LDPL for the radial distance d^i.

$$f_d^i = d_0^i 10^{\left(\frac{\overline{PL}(d) - \overline{PL}(d_0)}{10n}\right)} = d_j^i \tag{7}$$

However, in order to obtain radial distance from anchor node i d^i, PL exponent n should be estimated from the data collected during the offline phase. Let $\boldsymbol{m}^i = \{\widetilde{P}_r^{i,j}(d) | j = 1 \dots n_{loc}\}$ and $\boldsymbol{d}^i = \{d_j^i | j = 1 \dots n_{loc}\}$ be the RSS fingerprints acquired from anchor node i during surveying and corresponding distances from anchor node i, respectively. The estimated radial distance from anchor node i $\hat{d}^i$ can be obtained with an approximated propagation function $\hat{f}_d^i(m_j^i, n_i^*)$.

$$\hat{f}_d^i(m_j^i, n_i^*) = d_0^i 10^{\left(\frac{\widetilde{P}_t - \widetilde{P}_r^{i,j}(d) - \overline{PL}(d_0)}{10n_i^*}\right)} = \hat{d}_j^i \tag{8}$$

where n^* is the overall PL exponent which minimizes the sum of the absolute localization error.

$$n_i^* = \arg\min_n \sum_j |d_j^i - f_d^i(m_j^i, n)| \tag{9}$$

After obtaining the approximated propagation function, the measurements acquired from the anchor nodes are mapped to relative radial distances in order to distinguish the absolute position of the agent in the environment, which forms the online phase of the FIRLs.

III. Multifrequency Multistage Radiolocation System

This section explains Multifrequency Multistage Radiolocation System (MFMS) in greater detail. Akin to conventional FIRLs, MFMS consists of two main phases, i.e. online and offline phases. During the offline phase, RSS and Round Trip Time (RTT) fingerprints from all anchor nodes are collected at many locations in the environment. The measurements are then used to approximate the radio wave propagation function to localize the agent in an environment. The online phase, on the other hand, makes use of the approximated propagation function obtained in the former phase. However, one major difference between MFMS and conventional FIRL approaches is that MFMS employs two different types of radio modules in three different stages to infer the location of the agent. Another major difference of the proposed method is that the acquired measurements are regarded as sequences in order to create a temporal-coherence between consecutive estimations.

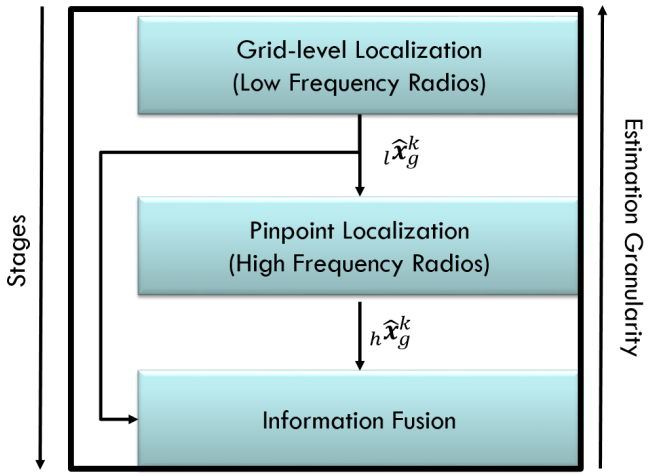

Fig. 2: MFMS Model: Grid-level localization stage infers the location of the agent in grid-level granularity represented as a probabilistic distribution over the localization environment $\boldsymbol{\Omega}$, while in Stage-2 the granularity of estimations are minimized to a point $\in \mathbb{R}^3$. In Stage 3, on the other hand, the grid-level estimation is fused with the point estimation of Stage 2.

Figure 2 shows the general layout of the proposed method. The first stage of MFMS, localizes the agent with a grid-level granularity solely based on measurements from 900 MHz radios. The grid-cell level estimations are represented with probabilistic belief function over localization environment. The second stage, on the other hand, utilizes 2.4 GHz radios and considers measurements as sequences in order to create a temporal-coherence between consecutive estimations. The radio wave propagation function is approximated within a Recurrent Neural Network framework due to its natural ability to employ sequences in the approximation. The third stage incorporates the finer-granularity location estimates based on measurements from 2.4 GHz with grid-level estimation into one final estimate.

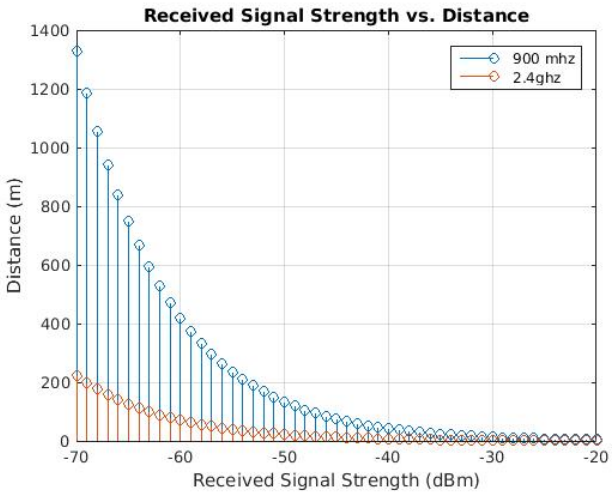

Fig. 3: RSS readings of two radio modules with same antenna characteristics are shown above. As the carrier frequency ($f_c = \frac{c}{\lambda}$) increases, the path loss shows the same trend. Thus, 900 MHz radios introduce a significantly bigger area of coverage comparing 2.4 GHz radios.

The main motivation behind employing multisource information is to exploit the diversity of the propagation characteristics of the different frequencies. As can be seen in the Equation (5) and Figure 3, the received power and separation distance shows a log-linear relationship. This figure implies two fundamental problems in radiolocation systems: The first problem is that as the carrier frequency increases path loss increases significantly, which limits the radio covarage and localization ability of the system in large environments. On the other hand, as the carrier frequency increases, the separation between two antennas, i.e. the anchor node and the target to be localized, can be identified with finer spatial resolution. Therefore, the trade-off between radio coverage and spatial localization resolution can be resolved by employing different frequencies in indoor localization systems by fusing the information acquired from the anchor nodes using different carrier frequencies. Thus, MFMS employs a radio module working at 900 MHz, and a radio module working at 2.4 GHz in each anchor node. Table I tabulates the specifications of the radios consisting in each anchor node, while Figure 4 demonstrates the details of the anchor nodes. In other words, wider spatial coverage is achieved by using low-frequency radio modules working at 900 MHz while finer spatial resolution provided by high-frequency radio modules working at 2.4 GHz frequency band.

A. Stage 1: Grid-cell Level Localization

This section covers the first stage of localization of the proposed method where the propagation of the radio waves is approximated in grid-level granularity and a special path loss exponent term is derived.

1) Grid-level Localization: During the online phase, MFMS first localizes the agent's vicinity with a grid-level

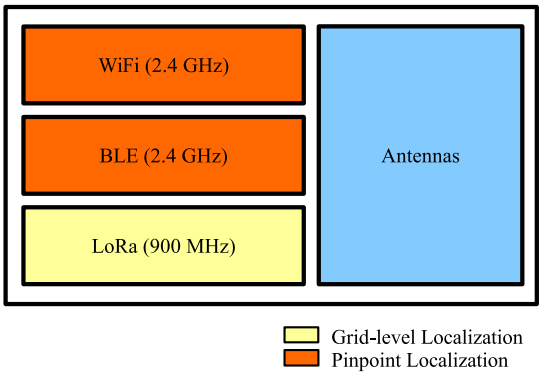

Fig. 4: MFMS Anchor Nodes

accuracy by employing a softmax classifier which is depicted in Figure 5. The classifier assigns a probability of the agent might reside to each grid cell given the acquired fingerprints obtained from low-frequency radio module. The reason MFMS solely employs low-frequency radio fingerprints in grid-level localization is that due to the higher probability of observing multiple modules in arbitrary positions in the environment, thanks to the smaller path loss they introduce. During the online phase, the estimated spatially-coherent path loss exponent, a set of physical parameter defining the radio wave propagation, is incorporated into the location estimation process in Stage-II.

2) Spatially-coherent Path Loss Exponent Estimation: LDPL model and its variants significantly suffers from dynamic environments and non-uniformly populated environments where some part of the environment is densely populated while other parts sparsely populated. As can be seen in Equation (9), LDPL model considers the environment as a whole while the path loss exponent, a scalar, is expected to approximate the propagation occurring...MFMS, however, does not consider the environment as a whole. Thus, we approach the problem by estimating a path loss exponent for different regions in the environment. In other words, the path loss exponent for MFMS is a function of the region at which the agent might reside. Therefore, the proposed system is able to tackle multi-modal propagation caused by non-uniform distribution of obstructions in the environment.

Let $\Omega = \{g_\theta | \theta = 1 \dots n_{grid}\}$ be the localization environment which is divided into n_{grid} number of grid cells g. Spatially-coherent path loss exponent $n_g^{*,i}$, which is the path loss exponent of anchor node i in grid cell g, can be formulated in least square sense, similar to LDPL model.

$$n_g^{*,i} = \arg\min_n \sum_{j_g} \left(d_{j_g}^i - f_d(m_{j_g}^i, n) \right)^2 \tag{10}$$

where $d_{j_g}^i$ and $m_{j_g}^i$ denote the radial distance between anchor node i and the measurement location within grid cell g, and the measurements acquired in grid cell g, while $f_d(\cdot)$ denotes the LDPL model. This estimation is conducted once during the offline phase from the collected fingerprints; while, during the online phase, the estimated spatially-coherent path loss exponents are chosen from $\boldsymbol{n}^{*,i} = \{n_g^{*,i} | g = 1 \dots n_{grid}\}$ according to the belief of the agent resides in the grid cell g.

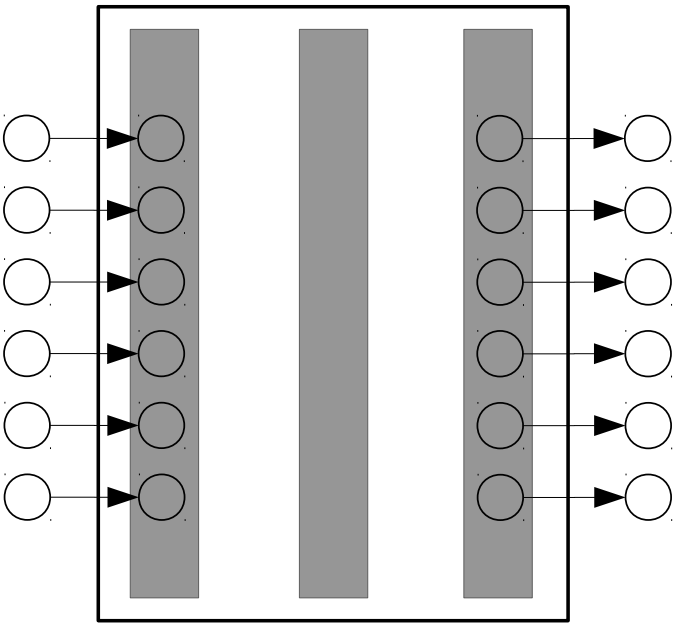

Fig. 5: The softmax classifier assigns weights for each anchor node based on the evidence representing the probability of residing in a grid cell g.

3) Anchor Node Selection: Based on the spatially-coherent path loss exponent, we can choose which anchor nodes are more useful and that.

B. Stage 2:Pinpoint Localization

This section gives details of the second stage of the MFMS which is the pinpoint localization. After obtaining the spatially-coherent path loss exponent corresponding to a grid cell, the agent is localized within the grid cell with finer spatial-resolution. This pinpoint localization process relies on the approximation joint propagation function of all the anchor nodes. Instead of independently modeling each anchor node, MFMS models all the propagation of functions jointly.

During the offline phase, the joint propagation function $\hat{g}_d(\cdot)$ is approximated with the collected fingerprints. The approximated joint propagation function is formulated as below.

$$\hat{g}_d(\boldsymbol{m}_j^{k-n_m:k}, \boldsymbol{n}_g^*) = \hat{\boldsymbol{x}} \tag{11}$$

where $\boldsymbol{m}_j^{k-n_m:k} \in \mathbb{R}^{n_{node} \times n_m}$, $\boldsymbol{n}_g^* \in \mathbb{R}_{node}^n$, and $\hat{\boldsymbol{x}}$ are the measurement vector acquired from all anchor nodes between time steps $k - n_m$ and k, the estimated path loss exponent vector of each anchor node for grid cell g and the estimated absolute position of the agent, respectively. As can be seen in Equation (11), the joint propagation function incorporates the measurements with the spatially-coherent path loss exponent vector so that the physical characteristics of the radio waves,

represented with the path loss vector, are enforced into the model as a parameter.

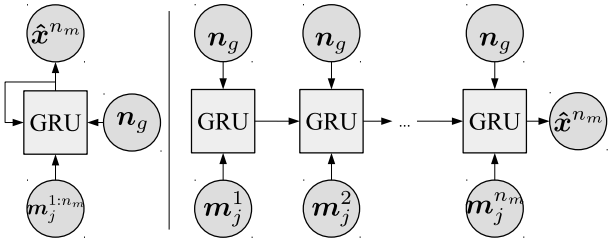

Fig. 6: Left: Folded Gated Recurrent Unit (GRU). Right: Unfolded GRU.

The propagation function of WiFi $\hat{g}_d^w(\cdot)$ and Bluetooth $\hat{g}_d^b(\cdot)$ anchors are approximated with two independent recurrent neural networks, consisting of three layers of GRU [2]. Unlike conventional Neural Network (NN) architectures, the recurrent neural networks are able to exploit information in form of sequences, i.e. the result of previous input affects the latter input. This ability is enables MFMS to exploit the temporal coherence of the radio waves and the physical limitations of the agents motion model. In other words, the estimation during the time step k should consider the estimation result of time step $k-1$. Figure 6 depicts a layer of GRU model in folded and unfolded representation. As can be seen in the figure, the GRU model recursively incorporates the each temporal slice of the input.

These functions are attained with a Stochastic Gradient Descent (SGD) based back-propagation algorithm. During the online phase of the MFMS, the approximated joint propagation functions are employed to estimate the location of the agent. Specifically, the pinpointing algorithm incorporates the spatially-coherent path loss exponent along with the weighted measurements to estimate $\hat{\boldsymbol{x}}^w$ and $\hat{\boldsymbol{x}}^b$, estimated positions by using WiFi measurements and Bluetooth measurements, respectively.

C. Stage 3:Information Fusion

This section of the paper further explains the Stage-III of the MFMS. The Stage-III is essentially an information fusion layer of the model where location estimates of WiFi and Bluetooth measurements are fused into one final entity. The incorporation of two estimates are achieved in the framework of a NN consisting of 3 layers. The network is in a gradually narrowing structure such that the first, second and last layer contain 8, 4, 2 neurons, respectively. Figure 7 demonstrates the Phase-III.

IV. Experimentation

A. Experimental Setup

This section will lay out the outline of the experimantation conducted. The experimentations are conducted on two different environments depicted on Figure 10. The first environment is a such-by-so area with no obstructions, while the second environment resides in a basement of Randolph Hall, Virginia Tech. The second environment consists of narrow corridors

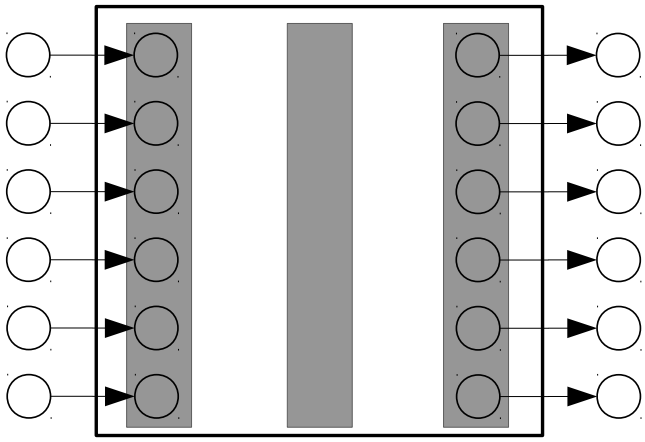

Fig. 7: Two location estimates of WiFi and Bluetooth approximations are fused with a 3 layered-NN.

TABLE I: The specifications of radios used in each anchor node

Property	2.4 GHz	900 MHz
Frequency [MHz]:	2400	900
Communication Bandwidth:	1-11 Mbps	10 Kbps
Transmission Power P_t [dBm]:	17	24
Reciever Sensivity [dBm]:	?	-101
Communication Range [m]:	$<$20	$>$100

which results in multipath propagation due to reflection and guiding effect of the walls. The circles on Figure 10 denote the location of the anchor nodes, while the grid size is set to be 50 centimeters, approximately 4 times of the wavelength of the WiFi and Bluetooth. Therefore, environment 1 and environment 2 consists of such and so grids, respectively. The efficacy of different stages of MFMS is investigated separately and all-combined. The first experimentation investigates the accuracy of grid-level localization which forms the Stage-I is examined in a statistical manner, while second experimentation investigates the accuracy of pinpoint localization stage. Later, the efficacy of the information fusion stage is investigated by comparing the results of individual WiFi and Bluetooth estimates to the fused estimates. The validity of MFMS is studied by repeating the experiments on two different environments of different sizes which introduces different level of obstructions.

1) Hardware: The anchor nodes used during the experimentations depicted on Figure 4. In detail, MFMS employes low-cost and off-the-shelf radio modules in the design of the anchor nodes. Each anchor node contains an XBee, referred as Long Range Radio (LoRa) working at 900 MHz, and a ESP32 containing a WiFi access point and a Bluetooth working at 2.4 GHz. Table I lays out the details of the individual module specification in detail. The mobile agent is equipped with an ESP32 and a low-cost Bluetooth module based on CSR8510 chipset.

2) Software: LoRa, WiFi, and Bluetooth measurements are collected with the module placed on the mobile agent, and transmitted to onboard computer via Serial communication protocol. The synchronization of the radios along with the parsing of the serial packets are implemented with ROS [3]. The approximation of the propagation function is achieved with the help of Keras [4] which uses Tensorflow [5] as the backend.

B. Results

Lorem ipsum dolor sit amet, consectetur adipisicing elit, sed do eiusmod tempor incididunt ut labore et dolore magna aliqua. Ut enim ad minim veniam, quis nostrud exercitation ullamco laboris nisi ut aliquip ex ea commodo consequat. Duis aute irure dolor in reprehenderit in voluptate velit esse cillum dolore eu fugiat nulla pariatur. Excepteur sint occaecat cupidatat non proident, sunt in culpa qui officia deserunt mollit anim id est laborum.

Fig. 8: The confusion matrix obtained during grid-selection.

Lorem ipsum dolor sit amet, consectetur adipisicing elit, sed do eiusmod tempor incididunt ut labore et dolore magna aliqua. Ut enim ad minim veniam, quis nostrud exercitation ullamco laboris nisi ut aliquip ex ea commodo consequat. Duis aute irure dolor in reprehenderit in voluptate velit esse cillum dolore eu fugiat nulla pariatur. Excepteur sint occaecat cupidatat non proident, sunt in culpa qui officia deserunt mollit anim id est laborum. Lorem ipsum dolor sit amet, consectetur adipisicing elit, sed do eiusmod tempor incididunt ut labore et dolore magna aliqua. Ut enim ad minim veniam, quis nostrud exercitation ullamco laboris nisi ut aliquip ex ea commodo consequat. Duis aute irure dolor in reprehenderit in voluptate velit esse cillum dolore eu fugiat nulla pariatur. Excepteur sint occaecat cupidatat non proident, sunt in culpa qui officia deserunt mollit anim id est laborum.

Lorem ipsum dolor sit amet, consectetur adipisicing elit, sed do eiusmod tempor incididunt ut labore et dolore magna aliqua. Ut enim ad minim veniam, quis nostrud exercitation ullamco laboris nisi ut aliquip ex ea commodo consequat. Duis aute irure dolor in reprehenderit in voluptate velit esse cillum dolore eu fugiat nulla pariatur. Excepteur sint occaecat

Fig. 9: Cumulative Distribution Function of the Localization Error in both environment: The red, blue and green lines depict localization error occurred when WiFi, Bluetooth and fused measurements are used in localization, respectively.

cupidatat non proident, sunt in culpa qui officia deserunt mollit anim id est laborum. Lorem ipsum dolor sit amet, consectetur adipisicing elit, sed do eiusmod tempor incididunt ut labore et dolore magna aliqua. Ut enim ad minim veniam, quis nostrud exercitation ullamco laboris nisi ut aliquip ex ea commodo consequat. Duis aute irure dolor in reprehenderit in voluptate velit esse cillum dolore eu fugiat nulla pariatur. Excepteur sint occaecat cupidatat non proident, sunt in culpa qui officia deserunt mollit anim id est laborum.

V. Conclusions and Future Work

1) P-1: Summary: Copy and paste from "this paper presents", paraphrase it, while summarizing it.
2) P-2: Results and Conclusions: Copy preface of numerical results section. For each results, add a resulting remark. Then conclude with a statement: "Results have demonstrated the effectiveness and applicability of the proposed approach."
3) P-3: Future work: This paper has focused on . . . and much work is still left open; describe a few future works.

Lorem ipsum dolor sit amet, consectetur adipisicing elit, sed do eiusmod tempor incididunt ut labore et dolore magna aliqua. Ut enim ad minim veniam, quis nostrud exercitation ullamco laboris nisi ut aliquip ex ea commodo consequat. Duis aute irure dolor in reprehenderit in voluptate velit esse cillum dolore eu fugiat nulla pariatur. Excepteur sint occaecat cupidatat non proident, sunt in culpa qui officia deserunt mollit anim id est laborum. Lorem ipsum dolor sit amet, consectetur adipisicing elit, sed do eiusmod tempor incididunt ut labore et dolore magna aliqua. Ut enim ad minim veniam, quis nostrud exercitation ullamco laboris nisi ut aliquip ex ea commodo consequat. Duis aute irure dolor in reprehenderit in voluptate velit esse cillum dolore eu fugiat nulla pariatur. Excepteur sint occaecat cupidatat non proident, sunt in culpa qui officia deserunt mollit anim id est laborum.

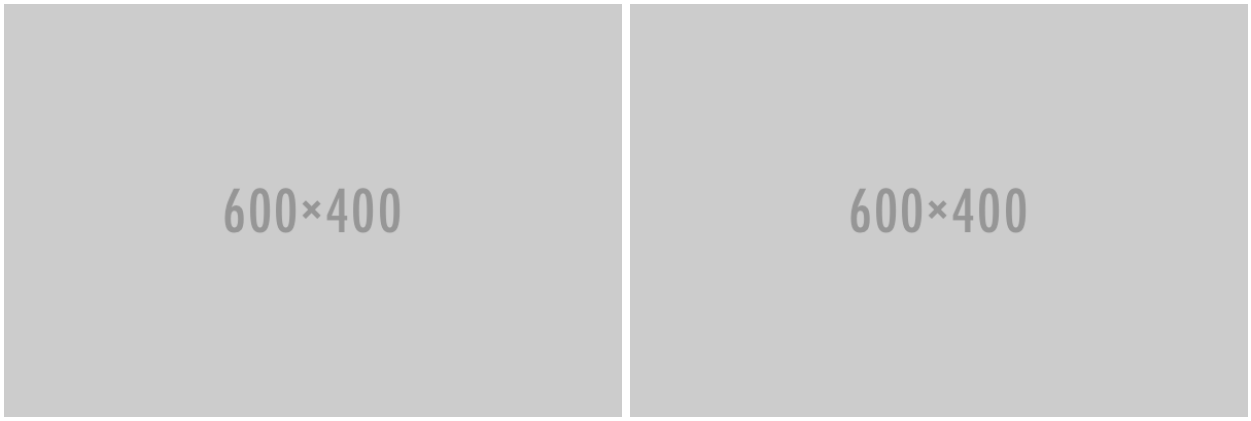

(a) Floor map of the first environment used in the experimentations

(b) Floor map of the first environment used in the

Fig. 10: The floor maps of the environments was conducted

Lorem ipsum dolor sit amet, consectetur adipisicing elit, sed do eiusmod tempor incididunt ut labore et dolore magna aliqua. Ut enim ad minim veniam, quis nostrud exercitation ullamco laboris nisi ut aliquip ex ea commodo consequat. Duis aute irure dolor in reprehenderit in voluptate velit esse cillum dolore eu fugiat nulla pariatur. Excepteur sint occaecat cupidatat non proident, sunt in culpa qui officia deserunt mollit anim id est laborum. Lorem ipsum dolor sit amet, consectetur adipisicing elit, sed do eiusmod tempor incididunt ut labore et dolore magna aliqua. Ut enim ad minim veniam, quis nostrud exercitation ullamco laboris nisi ut aliquip ex ea commodo consequat. Duis aute irure dolor in reprehenderit in voluptate velit esse cillum dolore eu fugiat nulla pariatur. Excepteur sint occaecat cupidatat non proident, sunt in culpa qui officia deserunt mollit anim id est laborum.

Lorem ipsum dolor sit amet, consectetur adipisicing elit, sed do eiusmod tempor incididunt ut labore et dolore magna aliqua. Ut enim ad minim veniam, quis nostrud exercitation ullamco laboris nisi ut aliquip ex ea commodo consequat. Duis aute irure dolor in reprehenderit in voluptate velit esse cillum dolore eu fugiat nulla pariatur. Excepteur sint occaecat cupidatat non proident, sunt in culpa qui officia deserunt mollit anim id est laborum. Lorem ipsum dolor sit amet, consectetur adipisicing elit, sed do eiusmod tempor incididunt ut labore et dolore magna aliqua. Ut enim ad minim veniam, quis nostrud exercitation ullamco laboris nisi ut aliquip ex ea commodo consequat. Duis aute irure dolor in reprehenderit in voluptate velit esse cillum dolore eu fugiat nulla pariatur. Excepteur sint occaecat cupidatat non proident, sunt in culpa qui officia deserunt mollit anim id est laborum.

ACKNOWLEDGMENTS

REFERENCES

[1] H. T. Friis, "A note on a simple transmission formula," *Proceedings of the IRE*, vol. 34, no. 5, pp. 254–256, 1946.

[2] K. Cho, B. Van Merriënboer, C. Gulcehre, D. Bahdanau, F. Bougares, H. Schwenk, and Y. Bengio, "Learning phrase representations using rnn encoder-decoder for statistical machine translation," *arXiv preprint arXiv:1406.1078*, 2014.

[3] M. Quigley, K. Conley, B. Gerkey, J. Faust, T. Foote, J. Leibs, R. Wheeler, and A. Y. Ng, "Ros: an open-source robot operating system," in *ICRA workshop on open source software*, vol. 3, no. 3.2. Kobe, Japan, 2009, p. 5.

[4] F. Chollet, "keras," https://github.com/fchollet/keras, 2015.

[5] M. Abadi, A. Agarwal, P. Barham, E. Brevdo, Z. Chen, C. Citro, G. S. Corrado, A. Davis, J. Dean, M. Devin, S. Ghemawat, I. Goodfellow, A. Harp, G. Irving, M. Isard, Y. Jia, R. Jozefowicz, L. Kaiser, M. Kudlur, J. Levenberg, D. Mané, R. Monga, S. Moore, D. Murray, C. Olah, M. Schuster, J. Shlens, B. Steiner, I. Sutskever, K. Talwar, P. Tucker, V. Vanhoucke, V. Vasudevan, F. Viégas, O. Vinyals, P. Warden, M. Wattenberg, M. Wicke, Y. Yu, and X. Zheng, "TensorFlow: Large-scale machine learning on heterogeneous systems," 2015, software available from tensorflow.org. [Online]. Available: http://tensorflow.org/